

## Research Article

**Cite this article:** Lovy J, Friend SE (2020). Black sea bass are a host in the developmental cycle of *Lernaenenicus radiatus* (Copepoda: Pennellidae): insights into parasite morphology, gill pathology and genetics. *Parasitology* **147**, 478–490. <https://doi.org/10.1017/S0031182019001781>

Received: 1 October 2019  
Revised: 10 December 2019  
Accepted: 16 December 2019  
First published online: 19 December 2019

**Key words:**

Black sea bass; genetics; gill pathology; *Lernaenenicus radiatus*; life cycle; Pennellidae.

**Author for correspondence:**

J. Lovy, E-mail: [Jan.Lovy@dep.nj.gov](mailto:Jan.Lovy@dep.nj.gov)

# Black sea bass are a host in the developmental cycle of *Lernaenenicus radiatus* (Copepoda: Pennellidae): insights into parasite morphology, gill pathology and genetics

J. Lovy  and S. E. Friend

Office of Fish and Wildlife Health and Forensics, N.J. Division of Fish and Wildlife, 605 Pequest Road, Oxford, NJ 07863, USA

**Abstract**

*Lernaenenicus radiatus*, a mesoparasitic pennellid copepod, has long been known in the northwest Atlantic with metamorphosed females infecting the muscle of marine fish. The study herein is the first to identify a definitive first host, black sea bass *Centropristis striata*, for *L. radiatus* supporting larval development to adults and sexual reproduction in the gills. This finding suggests a two-host life cycle for *L. radiatus*, with black sea bass as the first host. Heavy infections in the gill were associated with considerable pathology related to a unique and invasive attachment process that penetrated the gill and selectively attached to the gill filament cartilage. The morphology of the developing copepod was highly conserved with that of a related pennellid copepod, *Lernaecocera branchialis*, though was distinguished by the attachment process, unique pigmentation and other morphologic features described herein. Sequencing the small and large subunits of the ribosomal RNA and mitochondrial cytochrome c oxidase subunit I genes demonstrated *L. radiatus* to share closer identities with *Lernaecocera* and *Haemobaphes* spp. pennellid copepods rather than other *Lernaenenicus* spp. available in GenBank to date. Taxonomy of *L. radiatus* is discussed in relation to life cycles, tissue tropism, morphology and genetics of other closely related pennellid copepods.

**Introduction**

Black sea bass, *Centropristis striata*, is an economically important species throughout the northwest Atlantic, occurring from the Gulf of Maine down to Florida and are most abundant in the middle Atlantic Bight, where they are an equally vital species for commercial and recreational fishing. In 2017, commercial landings of black sea bass north of Cape Hatteras, North Carolina were 3.8 million pounds and recreational landings were estimated at 4.2 million pounds (ASMFC, 2018). Their high market demand has also led to them being a prime candidate species for aquaculture (Watanabe, 2011). Crustacean parasites have resulted in losses, including lost biomass from mortality and declined fish condition or unsightly injuries making fish unappealing for human consumption, in diverse marine fish species in the wild and in aquaculture (Kabata, 1970).

Copepods in the family Pennellidae are marine parasites requiring one or two hosts. Development to sexual maturity occurs on a single host, and females undergo metamorphosis into a much larger parasitic form in either the same host or in a new host (Lester and Hayward, 2006). For example, in northern Atlantic waters *Lernaecocera branchialis*, commonly known as cod worm, utilizes two different fish hosts, one supporting development from copepodids through four chalimus stages to adult copepods (Whitfield *et al.*, 1988). After sexual reproduction in the first host, the gills of a second host, most often an Atlantic cod *Gadus morhua*, are utilized by females for metamorphosis associated with severe enlargement of the parasite. Here the parasites posterior end and egg strings occur external to the fish from the gills and the parasite forms an attachment within the heart. Attachment and feeding on host blood from the heart causes reduced body condition, anaemia and mortality in the fish (Khan, 1988). Infections have been known to cause reductions in wild Atlantic cod (Jones and Taggart, 1998) and are a threat to marine aquaculture, particularly cod mariculture (Khan *et al.*, 1990). In the northwest Atlantic, *L. branchialis* occurs in northern waters, is rare in the mid-Atlantic Bight (Sherman and Wise, 1961) and likely absent in more southern waters. In the mid-Atlantic, the mesoparasitic pennellid copepod in the genus *Lernaenenicus* is most common.

The genus *Lernaenenicus* is composed of about 30 valid species and was established based on the characteristics of metamorphosed females, which infect diverse marine fish hosts (Walter and Boxshall, 2018). The full life cycle for many of the species in the genus has not yet been determined, except for *Lernaenenicus sprattae* and *Lernaenenicus ramosus* in Europe and Japan, respectively (Schram, 1979; Izawa, 2019). In the northwest Atlantic, three species of *Lernaenenicus* are believed to occur based only on the morphology of metamorphosed females

(Hogans, 2018). *Lernaeenicus radiatus* LeSueur 1824, which has previously only been documented in the metamorphosed female form, is described from at least 16 different marine fish hosts (Wilson, 1917; Voorhees and Schwartz, 1979; Hogans, 2018). Metamorphosed females have a long slender abdomen with egg strings noticeable externally to the fish, while internal to the fish they are often deeply embedded in the muscle by way of an anchoring process made up of radiating cephalic horns (Wilson, 1917; Hogans, 2018). Though the adult post-metamorphosed female form of this parasite has long been known in the northwest Atlantic, the larval and adult stages prior to female metamorphosis have remained unknown until the present study.

The pre-metamorphosed stages of pennellids look very similar among genera, particularly between *Lernaeenicus* and *Lernaeocera*, despite the metamorphosed females being quite distinct from each other. Similarity of the pre-metamorphosed stages has led to difficulties in species identification. Previously, copepods described from the gills of black sea bass were believed to be a species of *Lernaeocera* and later suggested to be *Lernaeenicus centropristi* (Pearse, 1947; Kabata, 1965). We show herein that the conspecific copepods from black sea bass gills are in fact developmental and adult stages of *L. radiatus*, documenting the first known initial host for this parasite. The reported similarities in *L. radiatus* and *L. branchialis* led us to more comprehensively compare their morphology and genetics in the present investigation. Further we note gill pathology related to *L. radiatus* infections in black sea bass and consider life cycle patterns, developmental morphology and genetics to better understand the relation of *L. radiatus* to other pennellid copepods.

## Materials and methods

### Black sea bass collection and sampling

Black sea bass ( $n = 30$ ) were collected off the coast of New Jersey in collaboration with the Bureau of Marine Fisheries, N.J. Division of Fish and Wildlife on July 18<sup>th</sup>, 2019 as part of the Ocean Stock Assessment Project. Fish were collected by biologists using pot traps set on an artificial reef located off the coast of southern New Jersey, USA (Lat 39°29.000', Long 74°10.000') (led by P. Clarke). This artificial reef was located about 10 km offshore with a depth of around 15 meters. Bottom water temperature on day of sampling was 11.4°C and was between 11.3 and 13.8°C in the month of July, as recorded by a temperature logger. The adult black sea bass, mean total length of  $27 \pm 3.5$  cm (range of 21–36.5 cm), were maintained on ice and transferred to the Pequest Fish Health Laboratory and examined for parasites within 24 h. Gills were examined and photographed using a Zeiss Stemi-2000 stereomicroscope (Carl Zeiss, Jena, Germany) with a ProgRes Gryphax Arktur CMOS digital camera (Jenoptik AG, Jena, Germany). Copepods were counted on the first gill arch from the left side of the fish to generate an estimate of infection intensity. Infected gill filaments were dissected and wet mounts were prepared to examine copepod attachment to the gill; to examine the fine structures of the parasites, copepods were removed from the gills and wet mounts were prepared of fresh specimens in seawater. Microscopic examination and photography were done using differential interference contrast on a Zeiss Axioplan 2 research microscope equipped with the above-mentioned digital camera. For molecular sample collection, copepods were removed from the gill and immediately frozen at  $-80^{\circ}\text{C}$ . The remaining gill arches were preserved in 10% neutral buffered formalin for histology.

For histology, tissues were routinely processed and  $4\mu\text{m}$  thick sections were cut and mounted on positively-charged slides. All tissue sections were stained with hematoxylin and eosin and select

slides were stained with a Luna stain (Luna, 1968), which is known to positively stain chitin, eosinophil granules, erythrocytes and cartilage.

### Reference samples of *Lernaeocera branchialis*

Reference samples of North American *L. branchialis* were collected off the coast of Newfoundland, Canada from adult lumpfish, *Cyclopterus lumpus*, to compare morphology and genetics. Lumpfish gills were provided by the Department of Ocean Sciences, Memorial University of Newfoundland, Canada (J. Fry and D. Boyce). Lethal gill samples were collected from a total of 23 lumpfish which were already being sampled as part of the cleaner fish broodstock program between July 8<sup>th</sup>–19<sup>th</sup>, 2019. Collection locations off the coast of Newfoundland, Canada included six fish from Baine Harbour, three from Champneys West (Trinity Bay), five from Gooseberry Cove (Trinity Bay), eight from Witless Bay and one from Holyrood (Conception Bay). The mean weight of the adult fish was  $2635 \pm 807$  g (range of 585–4154 g). The first gill arch was collected from each fish and preserved in 96% ethanol. The gill samples were then shipped to the Pequest Fish Health Laboratory, NJ USA, to screen for *L. branchialis*. Gills were screened and photographed using the above-mentioned stereomicroscope and camera. Lumpfish from Champneys West and Holyrood, Conception Bay, had gills moderately infected with *L. branchialis*, having about 50–75 copepods/gill arch. *Lernaeocera branchialis* was removed from the gills and replaced to fresh 96% ethanol and kept at  $-20^{\circ}\text{C}$  until further processing. Individual parasites were removed and wet mounts were prepared to examine microscopic structures using the above-mentioned microscope and camera. Histology was done on intact gill tissue containing parasites to better observe the attachment of the parasite to the gills; two gill samples that were moderately infected were rehydrated in a descending series of ethanols to water, followed by fixation for 24 h in 10% neutral buffered formalin and further processed for histology as described above.

For a reference genetic sample of *L. branchialis* from Europe, a tissue sample was taken from a museum specimen (# NTNU-VM-MI-73715) housed at the Norwegian University of Science and Technology, University Museum, Trondheim, Norway. This specimen was an adult metamorphosed female from the gill of Atlantic cod collected off the coast of Norway on July 17<sup>th</sup>, 2018 and preserved in 96% ethanol.

### Parasite measurements and drawings

Measurements were made on parasites from digital images using the ProgRes CapturePro Software (Version 2.10). Measurements of copepod total length were from the anterior tip of the cephalothorax, not including the second antennae, to the caudal terminus, not including setae of caudal rami. For consistency, measurements of females were done prior to severe elongation of the genital segment, since the genital segment may expand greatly during early metamorphosis which may start to occur prior to females dropping off the gills of black sea bass. Cephalothorax measurements included the same anterior portion back to the end of the carapace where the first set of swimming legs began and width measured at its greatest width, where the pigmentation occurred. The total length and width of antennae were included; for the second antennae the width was measured at the terminal segment at its greatest width. The diameter of the mouth tube was an average of two perpendicular measurements, since at times the mouth was not perfectly circular. A minimum of 30 parasites of both sexes was examined to verify structures. Drawings were made based on a series of digital images

taken at various focal planes of in-tact individuals using the Affinity Photo Software (version 1.6.9) on an iPad Pro.

### Polymerase chain reaction and sequencing

Five parasite samples were evaluated, including two *L. radiatus* from black sea bass, two *L. branchialis* from lumpfish and a single sample of *L. branchialis* from Atlantic cod in Norway. Deoxyribonucleic acid (DNA) was purified from parasite samples using the DNeasy blood and tissue kit automated on a QIAcube (QIAGEN) according to the manufacturer's instructions for extracting DNA from animal tissues. Samples were first completely lysed in a solution of 180  $\mu$ L Buffer ATL and 20  $\mu$ L proteinase K by bead beating for 2 min at 20 Hz and incubating for 2 h at 56°C. Polymerase chain reaction (PCR) primers for the amplification of the 18S and 28S rRNA genes were as reported by Song *et al.* (2008) and combined with general eukaryotic cell primers (Barta *et al.*, 1997; Whipps *et al.*, 2012; see Supplementary Table) to obtain nearly the full 18S sequence. Reactions were performed in 50  $\mu$ L volumes containing 3  $\mu$ L of template DNA, 1 $\times$  PCR buffer, 1.5 mM MgCl<sub>2</sub>, 0.2 mM each dNTP, 0.4  $\mu$ M of each primer and 5U Platinum Taq DNA Polymerase (Invitrogen) and topped up with molecular grade water. Amplification was completed on a Veriti thermocycler (Applied Biosystems) with initial denaturation at 94°C for 5 min, followed by 35 cycles of 94°C for 30 s, 54°C for 30 s and 72°C for 1 min, followed by a final extension at 72°C for 5 min. Products were sequenced using the amplification primers.

A 710 bp fragment of the mitochondrial cytochrome c oxidase subunit I (COI) gene was amplified using the primers reported by Folmer *et al.* (1994) (see Supplementary Table). Reaction mixture volumes were the same as those listed above for the PCR. Cycling conditions amplified the COI under the following parameters: initial denaturation at 94°C for 5 min, followed by 38 cycles of 94°C for 45 s, 48°C for 45 s and 72°C for 80 s, followed by a final extension of 72°C for 7 min. Products were sequenced using the amplification primers.

Products were visualized in 1.2% agarose E-gels (Invitrogen) containing SYBR Safe DNA gel stain and under ultraviolet light to confirm product size and purity. Samples were enzymatically purified with ExoSAP-IT (Affymetrix) and diluted to ~2 ng of DNA  $\mu$ L<sup>-1</sup> with molecular grade water plus 5  $\mu$ M of the respective amplification primer. Sequencing was done at GENEWIZ, Inc. (South Plainfield, NJ, USA) using ABI BigDye version 3.1 (Applied Biosystems), performed on an ABI 3730xl DNA analyser (Applied Biosystems). All sequences were checked for quality and base calls using Chromas (Version 2.6.6). The overlapping sequences were aligned using BioEdit (Version 7.2.5). Assembled sequences were queried in the National Center for Biotechnology Information's (NCBI) Basic Local Alignment Search Tool Nucleotide (BLASTn) to compare identities to other known species.

### Phylogenetic analysis

Mitochondrial COI nucleotide sequences were used to estimate the evolutionary history and phylogenetic relationships. A total of 23 sequences including *L. radiatus* and *L. branchialis* from this study, 20 other pennellid copepods from the NCBI database and *Bomolochus cuneatus* used as an outgroup, were represented. The sequences were aligned using Muscle and the best fit phylogenetic model was estimated using Mega X (Kumar *et al.*, 2018). The evolutionary history was inferred by using the Maximum Likelihood method and Hasegawa–Kishino–Yano model (Hasegawa *et al.*, 1985). There were a total of 698 positions in the final dataset. The tree with the highest log likelihood (−5604.55) is shown.

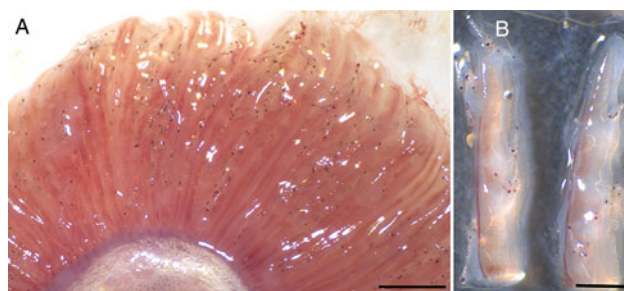


**Fig. 1.** Gills of black sea bass infected with *L. radiatus* (A) Gill with mature male and abundant female copepods. Scale 2 mm. (B) Two dissected gill filaments showing chalimus and adult copepods attached to the gill. Notice the pale areas around attached parasites indicative of epithelial hyperplasia and lamellar fusion. Scale 1 mm.

The percentage of trees in which the associated taxa clustered together in the bootstrap test (1000 replicates) was shown next to the branches; only bootstrap values over 0.50 were shown. Initial tree(s) for the heuristic search were obtained automatically by applying Neighbor-Join and BioNJ algorithms to a matrix of pairwise distances estimated using the Maximum Composite Likelihood approach, and then selecting the topology with superior log likelihood value. A discrete Gamma distribution was used to model evolutionary rate differences among sites [5 categories (+G, parameter = 0.4442)]. The rate variation model allowed for some sites to be evolutionarily invariable [(+I), 25.11% sites]. The tree is drawn to scale, with branch lengths measured in the number of substitutions per site. Codon positions included were 1<sup>st</sup> + 2<sup>nd</sup> + 3<sup>rd</sup> + noncoding.

## Results

### Gill observations and notes on *L. radiatus* development

All black sea bass gills were infected with *L. radiatus* with a mixture of developmental stages including chalimus stages, adult males and adult pre-metamorphic females. The copepods were found throughout the entire length of the gill filaments and did not have a preference for certain regions of the gill (Fig. 1A). The mean numbers of copepods on the first gill arch was 426 ± 514, with a range of 101–2946 copepods ( $n=30$ ). Grossly, gills appeared pale and epithelial hyperplasia was evident focally where parasites were attached (Fig. 1B). There was a total of four chalimus stages. The earliest stage observed was a stage I chalimus which had a relatively large cephalothorax in relation to the rest of the body (Fig. 2A). The paired first antennae were unsegmented with no rigidity and with small setae. The second antennae were non-chelate and held together anteriorly at the base of the attachment structure. Two sets of swimming legs were present, with a third set developing, though swimming setae were absent (Fig. 2A). Early formation of the attachment apparatus was observed at this stage (Fig. 2B). The main differences between the four chalimus stages were the further differentiation of swimming legs and development of plumes (Fig. 2C). When well-preserved, the chalimus stage was recognized by counting the remnants of previous larval cuticles around the attachment apparatus, which formed layers of hoods. These could not be confirmed in many of the stages. The stage IV chalimus had three previous hoods in addition to the intact one (Fig. 2D).

### Attachment of *L. radiatus* and associated gill pathology

The attachment apparatus was a long tubular appendage that selectively adhered to the cartilage of the gill filament. The

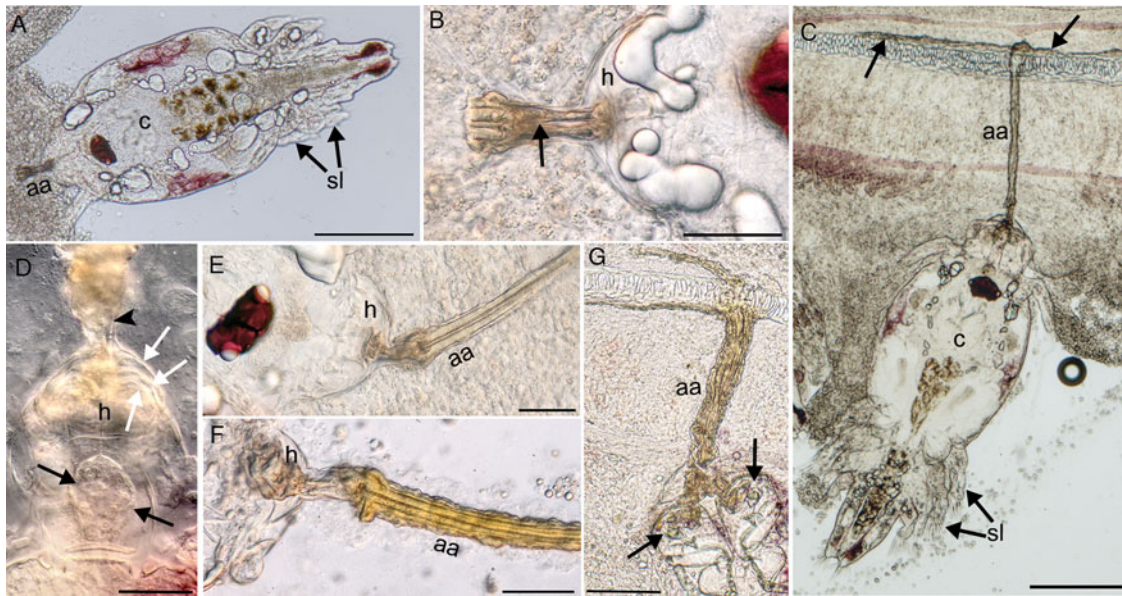


**Fig. 2.** Chalimus stages of *L. radiatus* in the gill of black sea bass showing the attachment apparatus (aa), hood (h), cephalothorax (c) and swimming legs (sl). (A) Chalimus I stage with large cephalothorax, swimming legs with no setae and the start of the attachment apparatus. Scale  $200\ \mu\text{m}$ . (B) Higher magnification of early attachment apparatus from (A) showing two parallel tubular structures originating from the hood, which appear to fuse (arrow) and then bifurcate. Scale  $50\ \mu\text{m}$ . (C) Chalimus IV stage with four swimming legs all containing setae and the attachment apparatus penetrating the gill and attaching to the cartilaginous gill filament. Notice the secretion over the cartilage to adhere the attachment (arrows). Scale  $200\ \mu\text{m}$ . (D) Attachment hood of a chalimus IV stage containing spherically arranged material (black arrows), one of the thin frontal filaments is visible (arrowhead) and the previous larval cuticles leaving three layers (white arrows) plus the intact hood. Scale  $50\ \mu\text{m}$ . (E) Attachment apparatus in chalimus II that is composed of two parallel tubular structures that bifurcate from the hood. Scale  $50\ \mu\text{m}$ . (F) Attachment apparatus of chalimus II with chitinous layers secreted over top of the tubular structures. Scale  $50\ \mu\text{m}$ . (G) Thickened tubular attachment apparatus in chalimus IV with multiple layers of secretions appearing to run through the second antennae (arrows). Scale  $100\ \mu\text{m}$ .

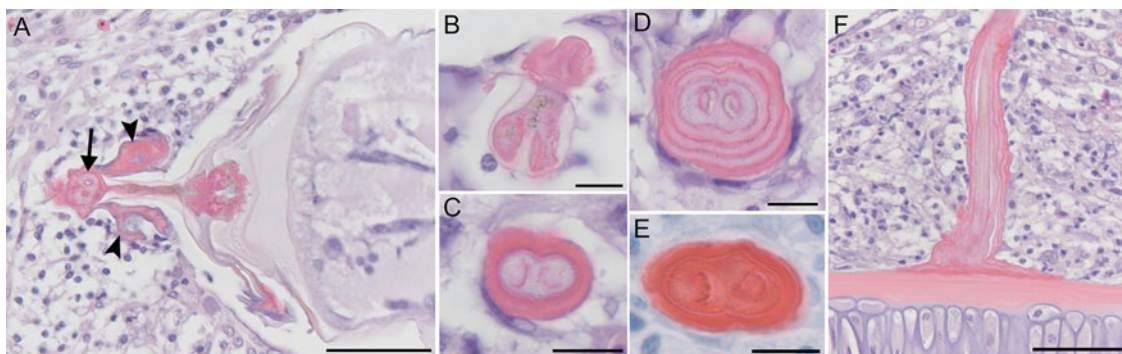


**Fig. 3.** Histology of the attachment apparatus of *L. radiatus* from gill of black sea bass; H&E stain in all except E which is stained with Luna. Scale (A, F)  $50\ \mu\text{m}$ ; (B–E)  $10\ \mu\text{m}$ . (A) Hood of a chalimus III stage showing tubular appendage, which in cross section (arrow) showed two tubular structures. Notice chitinous secretions on both sides (arrowheads). (B) Anterior segment of attachment apparatus showing bifurcation into two tubular structures. (C) Cross section of the early attachment apparatus containing two incomplete tubular structures surrounded by a single chitinous layer. (D) Cross section of a mature attachment apparatus containing two tubular structures in a light staining matrix surrounded by four layers of chitinous secretions. (E) Cross section of attachment apparatus staining positively with Luna stain. (F) Longitudinal section of the attachment to gill cartilage showing the central tubular structures surrounded by multiple layers of secretions.

synthesis of the attachment apparatus occurred from the hood located dorso-anteriorly between the first antennae and dorsal to the second antennae. The hood structure contained material in a spherical arrangement (Fig. 2D), which was likely the source from which the attachment apparatus was synthesized. Rarely, frontal filaments were seen originating from the spherical structure and leading to the base of the attachment apparatus (Fig. 2D). The attachment apparatus was present in the stage I chalimus, in which early development was observed. Two tubular structures running parallel to each other originated from the hood (Fig. 2B), which appeared to fuse with each other and then differentiate again into two tubular structures that extended into gill tissue until anchoring to the cartilage of the gill filament (Fig. 2C and E). A secretion of material occurred over top of the tubular elements to reinforce the attachment apparatus, giving it a

much thicker diameter (Fig. 2F and G). When the tubular attachment terminated at the gill cartilage, this secreted material covered the surface of the cartilaginous filament to adhere to the gill cartilage (Fig. 2G). The tubular attachment apparatus varied in length depending on proximity to the cartilage of the gill filament; the longest attachment apparatus observed was  $665\ \mu\text{m}$  in length. Females remained attached at least until copulation, evidenced by attached females having adhered sperm sacs to their genital segment. Adult males no longer had this attachment.

In H&E stained histology, the tubular structure of the attachment apparatus originated from the hood (Fig. 3A), from which it appeared to bifurcate into two tubular elements (Fig. 3B). In cross sections of the tubular attachment apparatus, it was composed of a central core containing two tubular structures in a lightly basophilic-stained matrix containing refractive material when

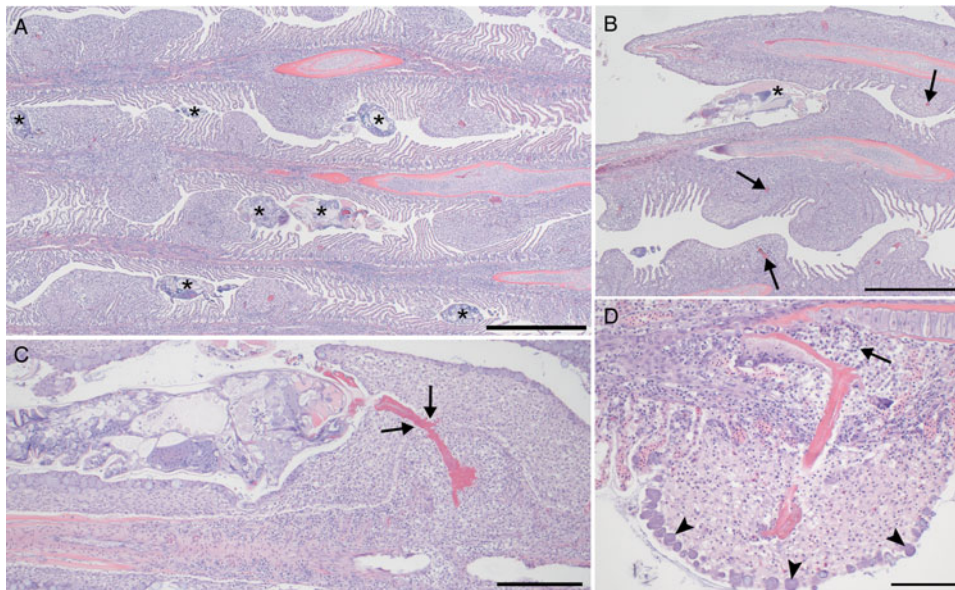


**Fig. 4.** Gill pathology related to *L. radiatus* in gills of black sea bass, H&E stain. (A) Gills with regions of lamellar fusion and epithelial hyperplasia reducing the lamellar surface, notice the sections of copepods (\*). Scale 500  $\mu\text{m}$ . (B) Copepod (\*) attached to the gill with lamellar fusion near attachment and in areas that contain sections of the attachment apparatus (arrows). Scale 200  $\mu\text{m}$ . (C) Attached female *L. radiatus* with the attachment apparatus breaching the basement membrane between the lamellar epithelium and the gill filament (arrows). Scale 200  $\mu\text{m}$ . (D) Attachment apparatus remaining in gill following detachment of copepod, notice the lamellar fusion with abundant mucus cells arranged in the periphery (arrowheads) and inflammatory cells lifting the attachment apparatus from the gill cartilage (arrow). Scale 200  $\mu\text{m}$ .

stained with H&E (Fig. 3C and D). The core was surrounded by 1 to 4 layers of eosinophilic material (Fig. 3C and D). The entire attachment apparatus stained positively with Luna stain, with the most intense staining occurring in the tubular structures in the core and the surrounding layers, indicating that these likely were composed of chitin (Fig. 3E). Luna stain is known to positively-stain erythrocytes, eosinophil granules, cartilage and chitin. In the longitudinal section, the core tubular structure was surrounded by multiple eosinophilic-staining layers, and the entire attachment terminated at the cartilage of the gill filament adhered by the secreted material (Fig. 3F).

The invasive attachment apparatus caused pathologic changes in the gill including epithelial hyperplasia and branchitis. In heavy infections, much of the gill tissue was impacted and a large portion of the lamellar surface area was reduced as a result of epithelial hyperplasia and lamellar fusion (Fig. 4A). Lamellar fusion occurred adjacent to attached parasites and around the attachment apparatus (Fig. 4B). The attachment apparatus breached the basement membrane separating the lamellae and the gill filament (Fig. 4C). An inflammatory infiltrate containing monocytes, macrophages and neutrophils occurred around the attachment in the gill filament, leading to swelling. Following detachment of adult males and females, the attachment apparatus remained in the gill, leaving the host to break down and eliminate the structure (Fig. 4D). Pathologic changes were directly associated with the parasite and attachment.

#### Morphology of adult *Lernaenicus radiatus* from black sea bass gills

The morphology of parasites was consistent with previous descriptions of the copepod reported by Kabata, (1965), with additional morphological features reported herein.

#### Adult female

Despite not having fully developed ovary, females at this stage were considered adults, since copulation occurred. This interpretation is similar to that of Sproston (1942) for *L. branchialis*. Copulation was

evidenced by adhered sperm sacs over the orifices posterior to the seminal receptacles of the genital segment. Females with attached sperm sacs were still attached to the gill *via* the frontal filament. Females were larger than males and with a more rectangular shaped cephalothorax (Fig. 5A). The genital segment of females had variable lengths. Measurements of copepods and select structures are summarized in Table 1. The longest total length of a post-mated female in the gill after the expansion of the genital segment was 3.5 mm. Pigmentation in fresh specimens was dark red in colour and occurred on the lateral sides of the carapace, base of the swimming legs, around the eyes and on the posterior end of the genital segment anterior to the caudal rami (Fig. 5). There were four pairs of swimming legs with the first two biramous and the second two uniramous. Leg 1 exopod with six plumose setae plus 1 spine, endopod with seven plumose setae; leg 2 was like leg 1; leg 3 uniramous with five plumose setae plus 1 spine; leg 4 with four plumose setae plus 1 spine (Fig. 5F–I). The first antennae were indistinctly 4-segmented. Setae occurred mainly on the anterior side (Fig. 5E). Second antennae were made up of three segments, including the chelae on the distal segment (Fig. 6A). The mouth cone was made up of a buccal tube comprised three rings as previously reported by Kabata, (1965). The diameter of the buccal tube was larger in the female than in the male (Fig. 6A and B, respectively). A band with blade-like lamellae at the base of the mouth cone was observed when the buccal tube was in profile. Notice the three teeth-like structures (arrow pointing to one of the teeth in Fig. 6C) that make up the lamellae. This was difficult to appreciate in most specimens. The maxilliped comprised two segments, with the basal segment armed with two spines and the distal segment with a curved tip (Fig. 6A). The cuticle of the genital segment was heavily wrinkled. The most obvious structures in the genital segment were the paired seminal receptacles. The ducts connecting the seminal receptacles to the external orifices were frequently looped over each other; in three females these were not looped over each other, though they were bent in an S-shape (Fig. 6D and E). Caudal rami were on both sides of the posterior tip, each had five short plumose setae, a pair on the lateral side and three medially (Fig. 5C).

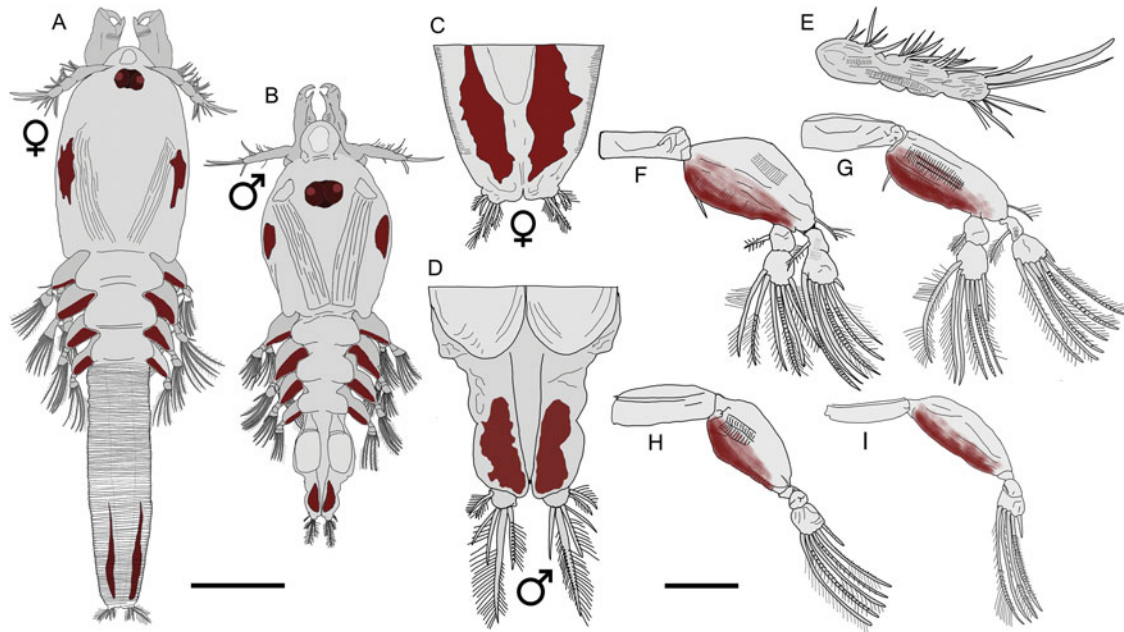


**Fig. 5.** Drawings representing *L. radiatus* from gills of black sea bass showing major morphological features and pigmentation. (A) Mature female; (B) mature male. Scale (A, B) 200  $\mu\text{m}$ , (C) Caudal end of female; (D) caudal end of male; (E) first antenna; (F) first swimming leg; (G) second swimming leg; (H) third swimming leg and (I) fourth swimming leg. Scale (C–I) 50  $\mu\text{m}$ .

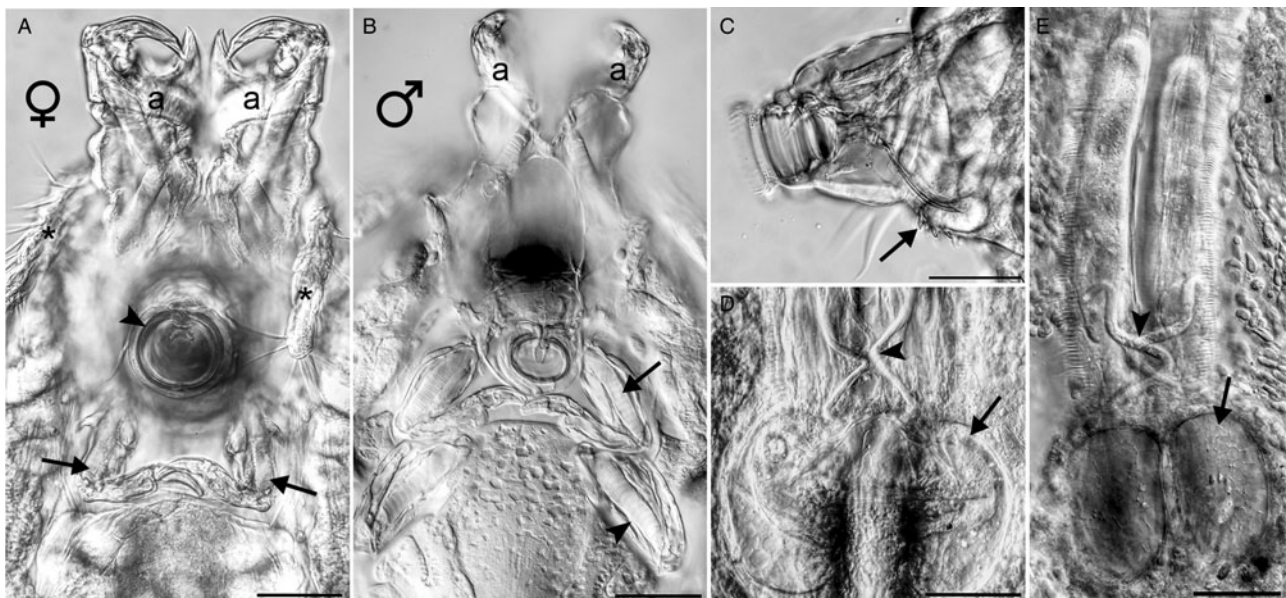


**Fig. 6.** *Lernaenicus radiatus* from gills of black sea bass. (A) Ventral view of female showing first antennae (\*), robust second antennae (a), mouth tube (arrowhead) and maxillipeds (arrows). (B) Ventral view of male showing mouth tube, first maxillipeds (arrow) and second maxillipeds (arrowhead). (C) Side view of mouth tube with a layer of teeth-like lamellae at the base (arrow). (D, E) Genital segment of female with two sperm sacs adhered near external orifices (arrows), ducts leading to seminal receptacles were often looped over each other and rarely not, but in an S configuration (arrowheads). Scale for all 50  $\mu\text{m}$ .

#### Adult males

The total length and cephalothorax dimensions were smaller than in the female (Table 1); cephalothorax was more rounded and eyes localized slightly more posterior than the female (Figs 5B). Similar dark red pigmentation as in the female (Fig. 5). Swimming legs and first antennae were like those in the female, though the first antennae were marginally longer in the male. The second antennae were chelate and much less robust, with nearly half the width as those in the female. Mouth cone and buccal tube like that of the female, though with a smaller diameter (Table 1). The first maxilliped was like that of the female except the basal

segment was not armed with spines. Unlike the female, males had a second pair of maxillipeds which were bi-segmented, with the terminal segment ending as a curved claw (Fig. 6B). The genital segment was much shorter than female and had paired extensions of the vas deferens directly anterior to the prominent paired spermatophore sacs. Caudal rami were more prominent and larger than in females each with a total of six plumose setae, also much longer and prominent than those in the female (Fig. 5D, compare to female caudal ramus in Fig. 5C). Each caudal ramus had paired shorter setae located

**Table 1.** Dimensions and standard deviation of select structures of *Lernaenicus (Le.) radiates* and *Lernaecocera (Lo.) branchialis* from gills of the first fish host. Dimensions and morphology are compared to previously reported *Lo. branchialis*, *Le. sprattae* and *Le. ramosus*. Some dimensions (\*) were taken based on parasite drawings.

Species/sex	Total length (mm)	Cephalothorax L × W (μm)	First antennae L × W	Second antennae L × W	Mouth tube diameter	Host/geographic range-distinguishing morphology	Reference
<i>Le. radiates</i> female	1.48 ± 0.3 (1.0–2.0) (n = 10)	560.7 ± 29.4 × 335.9 ± 5.3 (n = 10)	102.1 ± 11.2 × 22.6 ± 2.1 (n = 10)	127.2 ± 8.0 × 58.4 ± 3.3 (n = 10)	43.3 ± 6.4 (n = 4)	Black sea bass/NW Atlantic • Red pigment/mainly transparent • Small mouth tube • Teeth-like lamellae at base of mouth tube	This study
<i>Le. radiates</i> male	0.83 ± 0.04 (0.79–0.89) (n = 10)	375.5 ± 25 × 293.3 ± 18.1 (n = 10)	121.78 ± 9.4 × 22.1 ± 1.9 (n = 10)	94.7 ± 11.8 × 30.7 ± 4.8 (n = 10)	28.0 ± 1.0 (n = 4)		
<i>Lo. branchialis</i> NA female	1.96 ± 0.14 (1.83–2.25) (n = 9)	705.8 ± 18.8 × 501.7 ± 16.3 (n = 9)	142.2 ± 19.9 × 29.2 ± 3.5 (n = 7)	186.5 ± 13.4 × 91.4 ± 9.8 (n = 16)	74.27 (n = 1)	Lumpfish/NW Atlantic • Heavy black pigment dorsally • No teeth-like lamellae at base of mouth tube	This study
<i>Lo. branchialis</i> NA male	1.46 ± 0.05 (1.41–1.52) (n = 3)	642.8 ± 47.6 × 509.7 ± 18.9 (n = 3)	168.0 × 30.2 (n = 1)	197.0 ± 0.4 × 62.2 ± 17.7 (n = 2)	54.27 (n = 1)		
<i>Lo. branchialis</i> EU female	1.70 (1.25–1.91) (n = 2)	619 ± 0.05 No width	Dimensions not reported	Dimensions not reported	73 (n = 1)*	Flounder/NE Atlantic • Intense dark pigmentation • No teeth-like lamellae at base of mouth tube	Sproston (1942)
<i>Lo. branchialis</i> EU male	1.255 ± 0.12	517 ± 0.12 No width	Dimensions not reported	Dimensions not reported	73 (n = 1)*		
<i>Le. sprattae</i> female	1.43 ± 0.08 (1.25–1.61) (n = 30)	749 ± 27 × 394 ± 27 (n = 30)	L = 190	Max width = 190	168 ± 9.8 (n = 9)	Sprat, herring/NW Atlantic • Blue-black pigmentation • Prominent teeth-like lamellae at base of mouth tube • Very large mouth tube	Schram (1979)
<i>Le. sprattae</i> male	1.33 ± 0.03 (1.30–1.36) (n = 8)	738 ± 38 × 380 ± 38 (n = 8)	L = 190	Max width = 85	101 ± 3.4 (n = 9)		
<i>Le. ramosus</i> female	Not reported	Not reported	Not reported	Not reported	Not reported	Hong Kong grouper/Japan • Male with only three swimming legs • Oral cone different, projecting anteriorly	Izawa (2019)
<i>Le. ramosus</i> male	0.81–0.84 (n = 2)	450–470 × 360 (n = 2)	124.5 × 25.5*	60 × 60*	22.5*		

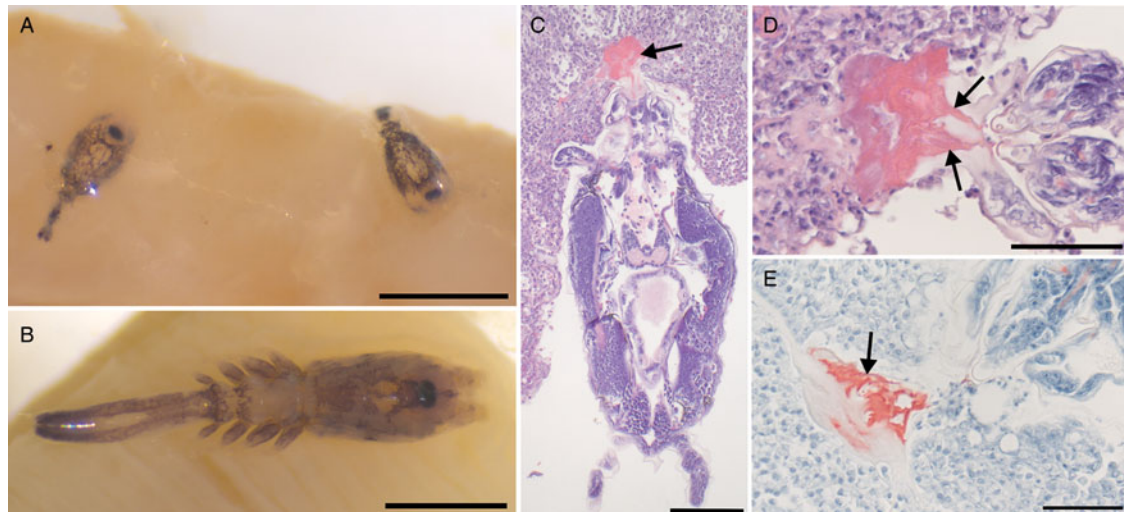


**Fig. 7.** *Lernaecera branchialis* from gills of lumpfish. (A) Chalimus stages and (B) adult females attached to the gill, both with heavy dorsal pigmentation composed of black pigment. Scale 500  $\mu\text{m}$ . (C–E) Histology showing attachment to the gill epithelium (arrows). Attachment is composed of two frontal filaments that widen in the tissue with secretion limited to epithelium. (C, D) H&E stain; (E) Luna stain; scale (C) 100  $\mu\text{m}$  and (D, E) 50  $\mu\text{m}$ .

laterally, and four medially with the central plumose setae considerably longer than the other three (Fig. 5D).

#### General morphology and gill attachment of *L. branchialis* in gills of lumpfish

*Lernaecera branchialis* development had been previously described from North America (Wilson, 1917) and the European side of the Atlantic (Sproston, 1942; reviewed by Brooker *et al.*, 2007), thus only general features and parasite dimensions were reported herein to compare to *L. radiatus* (Table 1). A primary focus was to detail the attachment of the parasite compared to *L. radiatus* in the current study. Gills of lumpfish contained chalimus stages and adult males and females, with an infection intensity of about 50–75 copepods within the first left gill arch. They occurred throughout the gill, though were primarily localized on the tips of gill filaments. The copepods were relatively heavily pigmented with a black pigment (Fig. 7A and B). Comparing total length, cephalothorax dimensions, second antennae and diameter of mouth tube, all were larger than that of *L. radiatus* (Table 1). Parasites and gill were fixed in 96% ethanol thus much of the gill colour had become pale. Despite this, attachment of *L. branchialis* was associated with a small paler area in the gill directly around the attachment. No filament or attachment apparatus was observed grossly or with a stereomicroscope. In histology, the chalimus stages were superficially attached to the gill, which had foci of epithelial hyperplasia associated with the attachment area. Attachment was comprised of two thin frontal filaments that widened within the tissue. From the frontal filaments there was a secretion of eosinophilic material that adhered the parasite within the gill epithelium. This attachment generally reached about 6–10 cells deep into the gill epithelium (Fig. 7C and D). The secreted material making up the attachment stained positively with Luna stain (Fig. 7E). The attachment organ and general morphology of gill were relatively well preserved despite initial fixation in 96% ethanol prior to formalin fixation. Shrinkage of gill epithelial cells was the main artifact caused by initial ethanol fixation.

#### Genetic characterization of *L. radiatus* and *L. branchialis*

##### Mitochondrial cytochrome *c* oxidase subunit I (COI)

*Lernaeniscus radiatus* from gills of black sea bass yielded a 678 nt sequence of the COI. GenBank accession numbers are stated in Table 2. This sequence shared identity with *L. radiatus* from

GenBank, 100% to MH235914 and 99.85% to MH235827, which corresponded to museum specimens of *L. radiatus* held in the Smithsonian National Museum of Natural History Invertebrate Zoology (USNM:IZ) collection deposited under catalog numbers 1463159 and 1463158, respectively. These specimens were collected from Chesapeake Bay, Maryland, USA as part of the Smithsonian Chesapeake Bay Barcode Initiative.

*Lernaecera branchialis* from lumpfish gills from Canada and *L. branchialis* from Atlantic cod from Norway were identical to each other. Nucleotide divergence in the COI between *L. radiatus*, *L. branchialis* and other closely related species was between 15–20%. Translated protein sequences were more conserved and demonstrated high identity of *L. radiatus* to *Haemobaphes* spp. and *L. branchialis* (98–100%) and less identity to other *Lernaeniscus* spp. (95–96%) (Table 2).

Phylogenetic analysis of the COI gene showed that the genus *Lernaeniscus* was polyphyletic. *Lernaeniscus radiatus* formed a grouping within a clade containing *Lernaecera* and *Haemobaphes* spp. (Fig. 8). *Lernaeniscus sprattae* and *L. ramosus* were closely related to each other in a grouping in a basal position compared to *L. radiatus* and *L. branchialis*. The clade for these species was poorly supported based on the low bootstrap values, and further taxon sampling will be necessary to better resolve the clades. Several species of *Lernaeniscus* (*L. seeri*, *L. alatus* and *L. hemirhamphi*) described from marine fish in India formed a clade basal to all other pennellid species included in the analysis (Fig. 8).

##### Ribosomal DNA (rDNA) sequences

GenBank accession numbers for sequences are noted in Tables 3 and 4. Identities showed that the 18S subunit was the most conserved gene between species and *L. radiatus* showed closest identity to *L. branchialis* (99.32%), and less identity to other *Lernaeniscus* spp. in GenBank (Table 3). *Lernaecera branchialis* from Canada and Norway were identical to each other. The 18S sequences from *L. branchialis* had 99.4% identity to a previous GenBank submission of *L. branchialis* from Europe accession # AY627030 (Table 3). The partial sequence of the 28S region was 760 bp long for both *L. radiatus* and *L. branchialis*. The highest identities were between *L. radiatus*, *H. pannosus* and *L. branchialis* (Table 4).

#### Discussion

Metamorphosed female forms of *L. radiatus* have been reported in at least 16 different fish hosts, some of which include

**Table 2.** Identities within COI nucleotide and translated protein sequences (bold) from the current study (\*) compared with closely related species. Percent identity is reported; GenBank accession numbers reported under species names. *Lernaeenicus* (*Le.*); *Lernaeocera* (*Lo.*) and identical (ID)

Sequence	<i>Le. radiatus*</i> MN520483	<i>Lo. branchialis*</i> MN520484	<i>Le. ramosus</i> LC317014	<i>Le. sprattae</i> KT209420	<i>H. pannosus</i> KR049062	<i>H. diceraus</i> LC179657						
<i>Le. radiatus*</i> MN520483	ID	<b>ID</b>	84.96	<b>98.22</b>	83.19	<b>96.00</b>	82.98	<b>94.98</b>	82.43	<b>100</b>	82.98	<b>99.04</b>
<i>Lo. branchialis*</i> MN520484	84.96	<b>98.22</b>	ID	<b>ID</b>	82.30	<b>94.67</b>	81.61	<b>93.61</b>	82.30	<b>98.45</b>	83.39	<b>99.04</b>
<i>Le. ramosus</i> LC317014	83.19	<b>96.00</b>	82.30	<b>94.67</b>	ID	<b>ID</b>	83.26	<b>97.26</b>	79.44	<b>96.39</b>	80.03	<b>95.19</b>
<i>Le. sprattae</i> KT209420	82.98	<b>94.98</b>	81.61	<b>93.61</b>	83.26	<b>97.26</b>	ID	<b>ID</b>	79.69	<b>95.36</b>	79.87	<b>94.23</b>
<i>H. pannosus</i> KR049062	82.43	<b>100</b>	82.30	<b>98.45</b>	79.44	<b>96.39</b>	79.69	<b>95.36</b>	ID	<b>ID</b>	87.83	<b>99.48</b>
<i>H. diceraus</i> LC179657	82.98	<b>99.04</b>	83.39	<b>99.04</b>	80.03	<b>95.19</b>	79.87	<b>94.23</b>	87.83	<b>99.48</b>	ID	<b>ID</b>

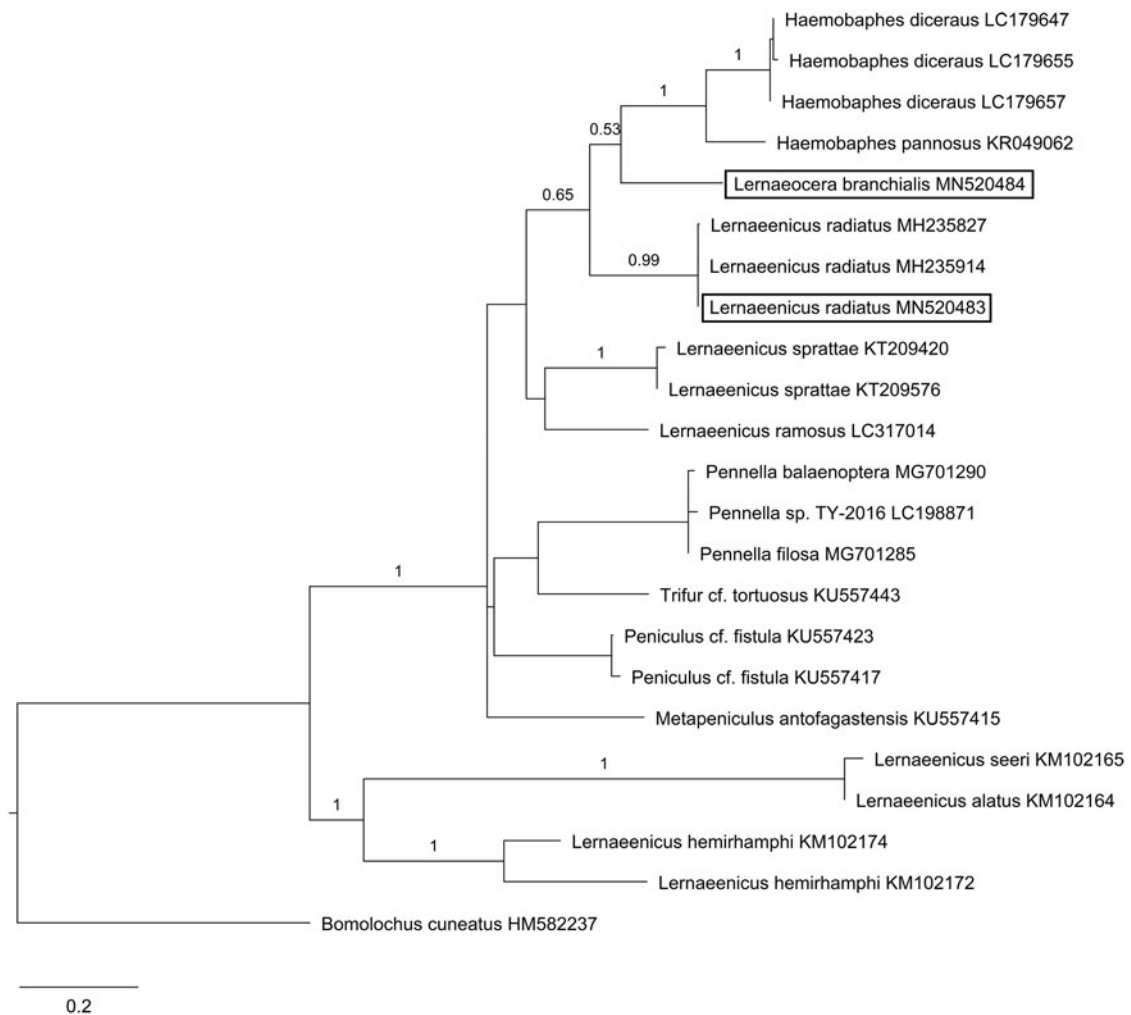


**Fig. 8.** Phylogenetic tree based on Maximum likelihood analysis of the COI gene showing *Lernaeenicus* is polyphyletic and that *L. radiatus* groups close to a clade containing *Lernaeocera* and *Haemobaphes* spp. Species from this study are boxed in. Bootstrap values above 0.50 are shown next to the branches.

Atlantic menhaden, *Brevoortia tyrannus*, Bay anchovy, *Anchoa mitchilli*, white perch, *Morone americana*, tomcod, *Gadus tomcod*, Atlantic croaker, *Micropogonias undulatus*, killifish, *Fundulus heteroclitus*, blueback herring, *Alosa aestivalis* and American eel, *Anguilla rostrata* (Wilson, 1917; Voorhees and Schwartz, 1979; Hogans, 2018). Until the present study, a host supporting

development and sexual reproduction of *L. radiatus* had not been identified. Some pennellid copepods utilize a two-host life cycle, a first host (definitive host) that supports copepod development and sexual reproduction and a second host supporting metamorphosis of females, while other pennellids complete their life cycle within a single host. The study herein was the

**Table 3.** 18S rDNA sequence identity table with sequences from this study (\*) compared to closely related species from GenBank. Percent identity is reported; GenBank accession numbers reported below species names. *Lernaenicus* (Le.); *Lernaocera* (Lo.) and identical (ID)

Sequence	<i>Le. radiatus*</i> MN523342	<i>Lo. branchialis*</i> MN523343	<i>Lo. branchialis</i> AY627030	<i>H. pannosus</i> KR048773	<i>Le. sprattae</i> MF077735
<i>Le. radiatus*</i> MN523342	ID	99.32	98.80	98.63	97.79
<i>Lo. branchialis*</i> MN523343	99.32	ID	99.43	98.93	98.06
<i>Lo. branchialis</i> AY627030	98.80	99.43	ID	98.46	98.07
<i>H. pannosus</i> KR048773	98.63	98.93	98.46	ID	97.15
<i>Le. sprattae</i> MF077735	97.79	98.06	98.07	97.15	ID

**Table 4.** 28S rDNA sequence identities from the current study (\*) compared to closely related species from GenBank. Percent identity is reported; GenBank accession numbers are reported below species names. *Lernaenicus* (Le.); *Lernaocera* (Lo.) and identical (ID)

Sequence	<i>Le. radiatus*</i> MN520221	<i>Lo. branchialis*</i> MN520222	<i>H. pannosus</i> KR048859	<i>Le. sprattae</i> MF077821	<i>Le. romosus</i> LC317015
<i>Le. radiatus*</i> MN520221	ID	96.05	96.44	93.22	91.86
<i>Lo. branchialis*</i> MN520222	96.05	ID	99.29	92.47	92.90
<i>H. pannosus</i> KR048859	96.44	99.29	ID	93.03	92.88
<i>Le. sprattae</i> MF077821	93.22	92.47	93.03	ID	90.21
<i>Le. romosus</i> LC317015	91.86	92.90	92.88	90.21	ID

first to identify the first (definitive) host for *L. radiatus*, which supports larval to adult copepod development and sexual reproduction. Gill infections of larval *L. radiatus* have not been previously reported in any other species, thus presently black sea bass is the only species known with developmental and adult stages of *L. radiatus* in the gill, suggesting that this parasite has a two-host life cycle starting with black sea bass. The host specificity of *L. radiatus* to black sea bass as a first host will still need confirmation by further examining gills of other fish species.

This was not the first description of this copepod in the gills of black sea bass, though identification of the species was difficult due to its remarkable similarity to *Lernaocera* and highly conserved morphology of the mature copepods in their first host. The conspecific parasite to the one herein was identified in North Carolina and described as *Lernaocera centropristi* (Pearse, 1947). Following this, Kabata, (1965) reevaluated the same parasite and concluded it more closely resembled *Lernaenicus* spp. and thus renamed it *L. centropristi*. We confirmed that this parasite from black sea bass is in fact a larval and adult form of *L. radiatus* prior to female metamorphosis. Linking the developmental stages in the black sea bass gill to *L. radiatus* was confirmed in the present investigation by sequencing the COI gene, which is the main target gene for barcoding of invertebrates (Folmer *et al.*, 1994; Raupach *et al.*, 2015; Castro-Romero *et al.*, 2016). This finding suggests that the species *L. centropristi* should be abolished, as these are in fact stages of *L. radiatus*. Future genetic studies and barcoding of diverse crustacea using the COI gene will be invaluable in linking the life cycle of species within the Pennellidae to better understand their life history.

A notable finding herein was the unique attachment apparatus for *L. radiatus* larvae in the gills, which had not been previously documented. Since larval development has not been described for many pennellid species, previous descriptions of the attachment apparatus from diverse species are lacking. Attachment of developing *L. branchialis* (Sproston, 1942) and *L. sprattae* (Schram, 1979) have been shown to be similar to each other, comprising of two frontal filaments that superficially attach to epithelium. These previous descriptions were from parasites separated from the gill tissue, making it difficult to note on the attachment to the host. For this reason, we investigated the attachment of *L. branchialis* intact within the gill by histology and confirmed that the parasite attached superficially in the epithelium by way of two thin frontal filaments and a secretion to reinforce the attachment. The attachment apparatus in *L. radiatus* formed a long tubular appendage that deeply penetrated the gills and selectively attached to the cartilage of the gill filament. The relevance for this major difference may be related to the activity and life history of the host fish species. Perhaps higher activity levels in black sea bass related to foraging and mating require *L. radiatus* to form a more secure attachment compared to that of *L. branchialis* in lumpfish and flounder. The cartilaginous gill filament is a stronger, more rigid structure for attachment compared to the gill epithelium which has a high cell turnover rate. With this notable difference in attachment, this is a useful morphological characteristic to make note of in future descriptions of pennellid copepods.

The invasive attachment of *L. radiatus* caused considerable gill pathology. Larval development of *L. branchialis* in lumpfish and flounder has been reported to have minimal health impacts on

their hosts despite heavy infections (Templeman *et al.*, 1976). This may be related to the superficial attachment within the epithelium and thus less detrimental pathology (Templeman *et al.*, 1976; current study). This contrasted to the more invasive attachment of *L. radiatus* in black sea bass gills which occurred throughout the entire gill, with attachment associated with epithelial hyperplasia, lamellar fusion and branchitis. With 100% prevalence and heavy infections ranging from hundreds to thousands of attached copepods per gill arch, the health impact caused by these copepods is an important consideration. Gills are a multi-functional organ with a high surface area responsible for respiration, osmoregulation and excretion of metabolic waste products (Speare and Ferguson, 2006). The fish collected in the study herein were not apparently ill and perhaps have a high tolerance to gill damage caused by these infections.

It is possible that gill damage induced by parasites may be overcome under normal metabolic processes in relatively good water quality. However, these infections may impact how fish handle environmental stressors and activity that requires a higher metabolic scope. This is particularly important for black sea bass populations, known to experience hypoxic or anoxic conditions in the coastal habitat during the summer (Hales and Able, 1995), which is when heavy infections with this parasite occurred in the present study. Other gill diseases in marine fish have been shown to impair gill function. For example, amoebic gill disease in Atlantic salmon results in decreased metabolic scope and compromises ion regulation (Hvas *et al.*, 2017). Additionally, metabolic scope is impaired by microsporidial gill infection in Atlantic cod (Powell and Gamperl, 2016). It has been shown that fish can overcome some of the negative effects of gill disease by increasing the efficiency of oxygen extraction and enhancing capacity for anaerobic metabolism (Powell and Gamperl, 2016). How *L. radiatus* impacts gill health of wild black sea bass populations is an important consideration and avoidance of this parasite in an aquaculture setting would be particularly important for maintaining optimal fish health.

Several morphologic features of the copepods have been described herein that were not previously shown and aid in distinguishing *L. radiatus* from other species. The most significant of these was the unique attachment apparatus discussed above. Additionally, the overall pigmentation of *L. radiatus* differed from other species in that the pigment was a dark-red colour, and generally there was less pigment making the parasite relatively translucent. We summarized the main distinguishing features and dimensions of select structures between *L. radiatus* and *L. branchialis* from this study compared to other *Lernaenicus* spp. from previous studies (Table 1). We also confirmed the finding from Kabata, (1965) showing that in females the ducts to the seminal receptacles often crossed over each other, which did not occur in *L. branchialis*. This does appear to be a distinguishing feature between *L. radiatus* and *L. branchialis*, though it may be related to the shifting of the seminal receptacles making the ducts cross over. Nonetheless, it is a feature not reported in *L. branchialis*.

Genetic comparisons herein showed *Lernaenicus* to be a polyphyletic genus and that *L. radiatus* had higher identity to *L. branchialis* and *Haemobaphes* spp. than to other *Lernaenicus* spp. The identical genetics of *L. branchialis* collected from Norway and Canada supports that these are the same species, as proposed by Kabata, (1961) who showed identical morphology in these, despite the geographic separation and different host preferences. The 18S rRNA gene, a highly conserved gene previously used to understand phylogeny of copepods (Khodami *et al.*, 2017), showed the smallest differences between the species herein. Interestingly, *L. radiatus* showed considerable divergence from *L. sprattae* (the only other species in the genus with 18S rDNA sequence available) with 2.21% divergence in

the sequence, whereas it only diverged by 0.68% from *L. branchialis* collected from Canada and Norway. The identities within the 28S rDNA sequences supported a similar pattern. The COI gene had the most representation for pennellid copepods because this is the target gene for barcoding of invertebrates (Folmer *et al.*, 1994; Raupach *et al.*, 2015) and it has been shown to be a useful marker for taxonomy within Pennellidae (Castro-Romero *et al.*, 2016). Because of high nucleotide divergence rates between species, we compared translated protein sequences, since amino acids are more highly conserved than nucleotides in evolution. Translated protein sequences supported the pattern of high identity of *L. radiatus* to *Haemobaphes* spp. and *L. branchialis*, while more diverged from the other *Lernaenicus* species. *Lernaenicus radiatus* formed a separate grouping from *L. sprattae* and *L. ramosus*, and both grouped separately from the *Lernaenicus* spp. described from India (Raja *et al.*, 2016). Considering that the morphology of metamorphosed females has historically been used for taxonomy, the polyphyletic phylogeny suggests that other characters must be used to understand the evolution and taxonomy of pennellid copepods.

Current taxonomy of pennellids based on the morphology of metamorphosed females (Wilson, 1917) has been out of necessity, since relatively few complete life cycles are known in this group. A difficulty in using metamorphosed females in taxonomy is the apparent variation of morphology in metamorphosed females even within individual species, as pointed out by Castro-Romero *et al.* (2016). This morphologic plasticity has been documented for *Lernaecocera* and has been attributed to host size and location of infection (Kabata, 1979; Van Damme and Ollevier, 1995). Similar morphologic plasticity had been reported for *L. radiatus* with the morphology of developing horns being influenced by the type of tissue infected, i.e. bony operculum vs muscle (Wilson, 1917; Hogans, 2018), thus it is common to see *L. radiatus* with less than the typical five horns. This plasticity in morphology makes it less useful for taxonomic descriptions and it appears that starkly different body forms can be a product of tissue tropisms. Future taxonomic studies carefully evaluating the male and pre-metamorphic females will be very useful, since these stages are more conserved and show less variability within species.

Life cycle patterns are important characters in the taxonomy of parasites. The life cycle of *L. radiatus*, including heavy infection of the gills of their first host, is like that described for *L. branchialis*, which heavily infect lumpfish gills in North America (Templeman *et al.*, 1976) and flounder gills in Europe (Whitfield *et al.*, 1988). The work herein suggests a two-host life cycle is likely for *L. radiatus* which includes black sea bass as a first host and a range of other marine fish species as second hosts. This is similar to the two-host life cycle in *L. branchialis*. Life cycles within the genus *Lernaenicus* have thus far shown to include only a single host, though this is only based on the known life cycles of two species. *Lernaenicus sprattae* completes its entire life cycle within the European sprat, *Sprattus sprattus* (Schram, 1979) and *L. ramosus* was shown to complete its entire life cycle within the Hong Kong grouper, *Epinephelus akaara* (Izawa, 2019). Both life cycles occurred within a single host species, though with a tissue tropism shift for the metamorphosis of the females. For *L. sprattae*, larval development occurred in the skin and fins and females migrated to the eye where metamorphosis occurred (Schram, 1979), whereas in *L. ramosus* larvae were found in gills and metamorphic females predominantly on the fins (Izawa, 2019). Clear differences may be seen in the utilization of hosts in the life cycle of pennellid copepods. One species, *Peniculus minuticaudae*, has been shown to complete its entire life cycle within a single host and without a change in tissue tropism (Ismail *et al.*, 2013). Future taxonomic revisions within pennellid copepods should focus on understanding life cycle patterns, morphology of adult stages prior to female

metamorphosis and genetic data to best understand the evolution of this group of copepods.

**Supplementary material.** The supplementary material for this article can be found at <https://doi.org/10.1017/S0031182019001781>.

**Acknowledgements.** We are grateful for the assistance of Peter Clarke and Greg Hinks from the Bureau of Marine Fisheries, N.J. Division of Fish and Wildlife, who provided the fish for this study, and Dr Ken Able and Maggie Shaw from the Rutgers University Marine Field Station. We also thank Danny Boyce, Jess Fry and Karstein Hårsaker for providing reference samples of *L. branchialis*. We'd like to thank Bridget Giblin and Vincent Nicoletta for assistance with fish sampling in the fish health lab. Lastly, we are grateful for the laboratory support from the Animal Health Diagnostic Laboratory, N.J. Department of Agriculture.

**Financial support.** Funding for this study was provided by the Federal Aid in Sport Fish Restoration Act (Project # FW-69-R-20) and the New Jersey Hunter and Anglers Fund.

**Conflict of interest.** None.

**Ethical standards.** Not applicable. Fish sampling was done in accordance with approved methods in the Wildlife and Sportfish Restoration Program, Fish and Wildlife Health Project.

## References

- Atlantic States Marine Fisheries Commission (ASMFC)** (2018) Black Sea Bass. <http://www.asmf.org/species/black-sea-bass> (Accessed 3 September 2019).
- Barta JR, Martin DS, Liberator PA, Dashkevich M, Anderson JW, Feighner SD, Elbrecht A, Perkins-Barrow A, Jenkins MC, Danforth HD, Ruff MD and Profous-Juchelka H** (1997) Phylogenetic relationships among eight *Eimeria* species infecting domestic fowl inferred using complete small subunit ribosomal DNA sequences. *Journal of Parasitology* **83**, 262–271.
- Brooker AJ, Shinn AP and Bron JE** (2007) A review of the biology of the parasitic copepod *Lernaocera branchialis* (L., 1767) (Copepoda: Pennellidae). *Advances in Parasitology* **65**, 297–341.
- Castro-Romero R, Montes MM, Martorelli SR, Sepulveda D, Tapia S and Martínez-aquino A** (2016) Integrative taxonomy of *Peniculus*, *Metapeniculus*, and *Trifur* (Siphonostomatoida: Pennellidae), copepod parasites of marine fishes from Chile: species delimitation analyses using DNA barcoding and morphological evidence. *Systematics and Biodiversity* **14**, 466–483.
- Folmer O, Black M, Hoeh W, Lutz R and Vrijenhoek R** (1994) DNA Primers for amplification of mitochondrial cytochrome *c* oxidase subunit I from diverse metazoan invertebrates. *Molecular Marine Biology and Biotechnology* **3**, 294–299.
- Hales LS, Able KW** (1995) Effects of oxygen concentration on somatic and otolith growth rates of juvenile black sea bass, *Centropristis striata*. In Secor DH, Dean JM and Campana SE (eds), *Recent Developments in Fish Otolith Research*. Belle W. Baruch Library in Marine Science 19. University of South Carolina Press, pp. 135–153.
- Hasegawa M, Kishino H and Yano T** (1985) Dating the human-ape split by a molecular clock of mitochondrial DNA. *Journal of Molecular Evolution* **22**, 160–174.
- Hogans WE** (2018) Functional morphology and structural variability in *Lernaenicus* (Copepoda: Pennellidae) parasitic on teleost fishes from the northwest Atlantic Ocean. *Comparative Parasitology* **85**, 13–26.
- Hvas M, Karlsbakk E, Mæhle S, Wright DW and Oppedal F** (2017) The gill parasite *Paramoeba perurans* compromises aerobic scope, swimming capacity and ion balance in Atlantic salmon. *Conservation Physiology* **5**, 1–12.
- Ismail N, Ohtsuka S, Maran BAV, Tasumi S, Zaleha K and Yamashita H** (2013) Complete life cycle of a pennellid *Peniculus Minuticaudae* Shiino, 1956 (Copepoda: Siphonostomatoida) infecting cultured threadsail filefish, *Stephanolepis cirrhifer*. *Parasite* **20**, 42.
- Izawa K** (2019) Redescription of *Lernaenicus ramosus* Kirtisinghe, 1956 (Copepoda, Siphonostomatoida, Pennellidae), with description of its male and the postnaupliar developmental stages. *Crustaceana* **92**, 119–128.
- Jones MEB and Taggart CT** (1998) Distribution of gill parasite (*Lernaocera branchialis*) infection in northwest Atlantic cod (*Gadus morhua*) and parasite-induced host mortality: inferences from tagging data. *Canadian Journal of Fisheries and Aquatic Sciences* **55**, 364–375.
- Kabata Z** (1961) *Lernaocera branchialis* (L.) a parasitic copepod from the European and the American shores of the Atlantic. *Crustaceana* **2**, 243–249.
- Kabata Z** (1965) Systematic position of the copepod *Lernaocera centropristi*. *Proceedings of the Zoological Society of London* **144**, 351–360.
- Kabata Z** (1970) Book I: Crustacea as enemies of fish. In Snieszko SF and Axelrod HR (eds), *Diseases of Fish*. Jersey City, NJ, USA: T.F.H Publications, pp. 1–171.
- Kabata Z** (1979) *Parasitic Copepoda of British Fishes*. London, UK: Ray Society.
- Khan RA** (1988) Experimental transmission, development, and effects of a parasitic copepod, *Lernaocera branchialis*, on Atlantic cod, *Gadus morhua*. *Journal of Parasitology* **74**, 586–599.
- Khan RA, Lee EM and Barker D** (1990) *Lernaocera branchialis*: a potential pathogen to cod ranching. *Journal of Parasitology* **76**, 913–917.
- Khodami S, McArthur JV, Blanco-Bercial L and Arbizu PM** (2017) Molecular phylogeny and revision of copepod orders (Crustacea: Copepoda). *Scientific Reports* **7**, 9164.
- Kumar S, Stecher G, Li M, Knyaz C and Tamura K** (2018) MEGA X: molecular evolutionary genetics analysis across computing platforms. *Molecular Biology and Evolution* **35**, 1547–1549.
- Lester RJG and Hayward CJ** (2006) Phylum Arthropoda. In Woo PTK (ed.), *Fish Diseases and Disorders. Volume 1 Protozoan and Metazoan Infections*, 2nd Edn. Oxfordshire, UK: CAB International, pp. 466–565.
- Luna LG** (1968) *Manual of Histologic Staining Methods of the Armed Forces Institute of Pathology*, 3rd Edn. NY, USA: Blakiston Division, McGraw-Hill Inc.
- Pearse AS** (1947) Parasitic copepods from Beaufort, North Carolina. *Journal of the Elisha Mitchell Scientific Society* **63**, 1–16.
- Powell MD and Gamperl AK** (2016) Effects of *Loma morhua* (Microsporidia) infection on the cardiorespiratory performance of Atlantic cod *Gadus morhua* (L.). *Journal of Fish Diseases* **39**, 189–204.
- Raja K, Saravanakumar A, Gopalakrishnan A, Vijayakumar R, Hwang UW and Maran BAV** (2016) The genus *Lernaenicus* Lesueur (Copepoda, Siphonostomatoida, Pennellidae) in India: a checklist with notes on its taxonomy and ecology. *Zootaxa* **4174**, 192–211.
- Raupach MJ, Barco A, Steinke D, Beermann J, Laakmann S, Mohrbeck I, Neumann H, Kihara TC, Pointner K, Radulovici A, Segelken-Voigt A, Wesse C and Kneibelsberger T** (2015) The application of DNA barcodes for the identification of marine crustaceans from the North Sea and adjacent regions. *PLOS ONE* **10**, e0139421.
- Schram TA** (1979) The life history of the eye-maggot of the sprat *Lernaenicus sprattae* (Sowerby) (Copepoda, Lernaoceridae). *Sarsia* **64**, 279–316.
- Sherman K and Wise JP** (1961) Incidence of the cod parasite *Lernaocera branchialis* L. in the New England area, and its possible use as an indicator of cod populations. *Limnology and Oceanography* **6**, 61–67.
- Song Y, Wang GT, Yao WJ, Gao Q and Nie P** (2008) Phylogeny of freshwater parasitic copepods in the Ergasilidae (Copepoda: Poecilostomatoida) based on 18S and 28S rDNA sequences. *Parasitology Research* **102**, 299–306.
- Speare DJ and Ferguson HW** (2006) Gills and Pseudobranchs. In Ferguson HW (ed.), *Systemic Pathology of Fish: A Test and Atlas of Normal Tissues in Teleosts and Their Responses in Disease*. London, UK: Scotian Press, pp. 24–63.
- Sproston NG** (1942) The developmental stages of *Lernaocera branchialis* (Linn.). *Journal of the Marine Biological Association of the United Kingdom* **25**, 441–466.
- Templeman W, Hodder VM and Fleming AM** (1976) Infection of lumpfish (*Cyclopterus lumpus*) with larvae and of Atlantic cod (*Gadus morhua*) with adults of the copepod, *Lernaocera branchialis*, in and adjacent to the Newfoundland area, and inferences therefrom on inshore-offshore migrations of cod. *Journal of the Fisheries Research Board of Canada* **33**, 711–731.
- Van Damme PA and Ollevier F** (1995) Morphological and morphometric study of crustacean parasites within the genus *Lernaocera*. *International Journal for Parasitology* **25**, 1401–1411.
- Voorhees JT and Schwartz FJ** (1979) Attachment site, seasonality, and effects of the parasitic copepod *Lernaenicus radiatus* on two estuarine fishes in the Cape Fear River, North Carolina. *Transactions of the American Fisheries Society* **108**, 191–196.
- Walter TC and Boxshall G** (2018) World of copepods database. *Lernaenicus* Lesueur, 1824. Accessed at: <http://www.marinespecies.org/copepoda/aphia.php?p=taxdetails&id=135644> on 2019-12-02.
- Watanabe WO** (2011) Species profile: black sea bass. *Southern Regional Aquaculture Center* 7207, <https://agrifilecdn.tamu.edu/fisheries/files/2013/09/SRAC-Publication-No.-7207-Species-Profile-Black-Sea-Bass.pdf> (Accessed 3 September 2019).

- Whipps CM, Fournie JW, Morrison DA, Azevedo C, Matos E, Thebo P and Kent ML** (2012) Phylogeny of fish-infecting *Calyptospora* species (Apicomplexa: Eimeriorina). *Parasitology Research* **111**, 1331–1342.
- Whitfield PJ, Pilcher MW, Grant HJ and Riley J** (1988) Experimental studies on the development of *Lernaeocera branchialis* (Copepoda: Pennellidae): population processes from egg production to maturation on the flatfish host. *Hydrobiologia* **167/168**, 579–586.
- Wilson CB** (1917) North American Parasitic copepods belonging to Lernaeidae, with a revision of the entire family. *Proceedings US National Museum* **53**, 2194.